Proceedings of the Estonian Academy of Sciences
2025, **74**, 4, 525–538

https://doi.org/10.3176/proc.2025.4.06

www.eap.ee/proceedings
Estonian Academy Publishers

MATHEMATICAL PHYSICS, GENERAL RELATIVITY

RESEARCH ARTICLE

Received 31 January 2025
Accepted 14 April 2025
Available online 16 October 2025

Keywords:
Binet's equation, numerical integration, precession of Mercury's orbit, perturbational methods

Corresponding author:
Matti Selg
mselg@ut.ee

Citation:
Selg, M. 2025. Simple and reliable analytic approximation to the numerical solution of the relativistic Binet's equation: an application to Mercury. *Proceedings of the Estonian Academy of Sciences*, **74**(4), 525–538.
https://doi.org/10.3176/proc.2025.4.06

Simple and reliable analytic approximation to the numerical solution of the relativistic Binet's equation: an application to Mercury

Matti Selg

Institute of Physics, University of Tartu, W. Ostwaldi 1, 50411 Tartu, Estonia

ABSTRACT

The nonlinear trajectory equation (Binet's equation) for a particle in a relativistic force field can only be solved numerically or, alternatively, by using a perturbational solution scheme. The latter approach was successfully applied by Albert Einstein in 1915 to deduce the celebrated formula that explains the anomalous precession of the perihelion of Mercury. In this article, Binet's equation for Mercury is solved numerically to a high degree of accuracy (16 decimal digits). This is a necessary comparison basis for the main goal of this work – to deduce a simple analytic formula that perfectly reproduces the real relativistic trajectory. Several analytical models are proposed, and the main goal has been indeed achieved. Moreover, the fitting parameters for model D described in Section 3 can be obtained independently of the solution of Binet's equation. Thus, we can say that the highly accurate relativistic trajectory (the largest discrepancy being about 30 cm) can be obtained without actually solving the nonlinear differential equation for this trajectory.

1. Introduction

The trajectory of a particle in a central force field can be deduced from Newton's second law for the radial motion:

$$m \cdot \left(\ddot{r} - r\dot{\theta}^2\right) = F(r) = -\frac{\partial V(r)}{\partial r}, \tag{1}$$

where $V(r)$ is the particle's potential energy. Changing the variable to $u = 1/r$ and using the law of conservation of the angular momentum

$$mr^2\dot{\theta} = L, \tag{2}$$

(1) transforms to

$$\frac{d^2u}{d\theta^2} + u = -\frac{Fm}{L^2u^2}, \tag{3}$$

which is more convenient for solving and is known as Binet's equation [1]. In fact, however, it was substantially given already in Newton's *Principia* [2] (Book I, II and III) (see [3], p. 78, for comments).

Newton's theory of gravitation has been remarkably successful. However, the pure Newtonian force $F \sim r^{-2}$ predicts a spatially fixed and closed elliptical orbit for a planet, which is not quite correct. Indeed, the very slow but still measurable precession of the orbits of planets is a well-known phenomenon. For example, the advance of Mercury's perihelion (as seen from Earth) has been determined to be 5600 arc seconds per century. The effect is mainly caused by gravitational perturbations from all other planets, which can be counted in terms of Newton's theory of gravity. This way, one can explain the shift of $5557''$, but there remains a discrepancy of $43''$ per century that cannot be accounted for by using Newton's theory.

The problem has been solved by the general theory of relativity, which introduces a slight correction to Newton's theory – a small force component that varies as $1/r^4$ $(= u^4)$. In 1915, Albert Einstein derived a formula for the anomalous perihelion shift for one period [4], p. 839, which was one of the major triumphs of the general theory of relativity:

$$\Delta = \frac{24\pi^3 a_\varepsilon^2}{T^2 c^2 (1 - \varepsilon^2)}. \tag{4}$$

Here, $c = 299792458$ m/s is the speed of light in vacuum, $T = 7.6005 \cdot 10^6$ s is the orbital period of Mercury, $a_\varepsilon = 5.7909 \cdot 10^{10}$ m is the length of Mercury's semimajor axis, and $\varepsilon = 0.2056$ is the orbit's eccentricity [6]. The predictions of (4) for Mercury are in very good agreement with the observational data. In fact, however, this is an approximate formula, which can be improved by using elliptic integrals [5].

In this paper, we are not going to discuss the physical content of Einstein's celebrated formula (4), but we will concentrate on the overall relativistic orbit, which can be obtained by solving the relativistic Binet's equation [7], p. 196, [8], p. 313, [9]

$$\frac{d^2u}{d\theta^2} + u = A + Bu^2, \; A \equiv \frac{GMm^2}{L^2}, \; B \equiv \frac{3GM}{c^2}, \tag{5}$$

where G is the gravitational constant, while M and m are the solar mass and Mercury's mass, respectively. Equation (5) is based on the Schwarzschild solution [10] to Einstein's field equations.

In principle, the same approach can be applied to any celestial body, but here the focus is put on the trajectory of Mercury. Our main goal is to find a simple analytic approximation to the real relativistic trajectory. Obviously, this only makes sense if the following preconditions are fulfilled:

1. The relativistic Binet's equation is solved very accurately. To be more specific, the accuracy of at least 16 decimal digits must be guaranteed.
2. The analytic approximation is highly reliable, so that the corresponding trajectory is almost indistinguishable from the true solution of the relativistic equation.
3. All parameters of the desired analytic formula are uniquely fixed by the basic parameters A and B of the relativistic equation.

To achieve the main goal, we have to fix the parameters A and B with the precision that matches the accuracy of computations. Thus, the following dimensionless values have been fixed and will be used for these parameters [11]:

$$A = \frac{GMm^2 a_p}{L^2} = 0.8294405557533, \tag{6}$$

$$B = \frac{3GM}{a_p c^2} = 9.6302165378 \cdot 10^{-8}. \tag{7}$$

Here, $a_p = 46001136.69$ km is the perihelion distance of Mercury [12,13].

Comment. One may suspect that too many digits are given in (6) and (7). Indeed, the parameters A and B are not known with such accuracy. However, in order to make a reliable comparison between the highly accurate numerical solution and its analytic approximation, the basic parameters must be fixed and treated as being exact (see [11] for more details).

The nonlinear equation (5) cannot be solved analytically. However, one can apply the same perturbational approach that was used to derive (4). The first-order perturbational solution to (5) is sufficient for our purposes, and it reads [14], p. 101, [7], p. 198:

$$u(\theta) = A_0 \cos(k\theta) + B_0, \tag{8}$$

where the parameters

$$A_0 = 1 - A, \; B_0 = A \tag{9}$$

and

$$k = 1 - AB = 0.999999920123 \tag{10}$$

are determined by the basic parameters A and B, as needed. On the other hand, A_0 and B_0 can be related to the perihelion (a) and the aphelion (b) of the trajectory given by (8):

$$A_0 = \frac{b - a}{2ab}, \; B_0 = \frac{a + b}{2ab}. \tag{11}$$

An important point is that (8) is, in fact, the **exact solution** of Binet's equation for a central potential of a different (nonrelativistic) type, namely [11]

$$u''(\theta) + u(\theta) = \frac{m}{L^2}\left(a_1 + 2a_2 u\right), \tag{12}$$

where

$$a_1 = \frac{L^2}{m} \cdot A \cdot (1 - AB) = GMmk^2 \tag{13}$$

and

$$a_2 = \frac{L^2}{2m} \cdot AB \cdot (2 - AB) = \frac{L^2}{2m}\left(1 - k^2\right).$$

Thus, as the result of the described perturbational procedure, the relativistic central force $F \sim r^{-4}$ is replaced with an effective $F \sim r^{-3}$ force. Note that the first term on the right side of (5) is also slightly modified: A transforms to Ak^2. It is easy to be convinced that (8) is the solution of equation (12). Moreover, it also correctly predicts the anomalous shift of Mercury's perihelion. Indeed, using (6), (7) and (10), we get

$$\Delta = \frac{2\pi}{1 - AB} - 2\pi = 2\pi \cdot \left(\frac{1}{k} - 1\right) = 5.01882 \cdot 10^{-7} \text{ rad/orbit}, \tag{14}$$
$$\Delta_c = 42.9807'' \text{ per century.}$$

The result is in good agreement with Einstein's formula (4), as well as with the observational data and the predictions of computer simulations [12]. It is therefore expected that (8) approximates the overall relativistic trajectory with reasonable accuracy. Indeed, the largest discrepancy, which shows up at Mercury's aphelion, is about 14 km [11]. However, formula (8) is only the first step towards the main goal mentioned above. The next steps will be described in the next sections.

2. Solution of the relativistic Binet's equation

2.1. Preliminary steps

Equation (5) can be integrated numerically using a high-quality online service [15]. However, to ensure the utmost accuracy, we prefer to solve the equivalent first-order equation, which reads [11]:

$$\begin{aligned} u'^2 &= (1 - u)\left[u + 1 - 2A - \frac{2B}{3}\left(u^2 + u + 1\right)\right] \rightarrow \\ u' &= -\sqrt{(1 - u)\left[u + 1 - 2A - \frac{2B}{3}\left(u^2 + u + 1\right)\right]} \end{aligned} \tag{15}$$

and can be transformed to

$$\frac{d\theta}{du} = -\frac{1}{\sqrt{(1 - u)\left[u + 1 - 2A - \frac{2B}{3}\left(u^2 + u + 1\right)\right]}}, \tag{16}$$

where we took into account that $u' < 0$. From here on, the perihelion distance is chosen to be the unit of length, i.e. $a_p = 1$. Equations (15) and (16) are related to the perihelion where $u = 1$ and $u' = 0$. An analoguous pair of equations can be related to the aphelion where also $u' = 0$, but $u = u_\varphi \neq 1$. The aphelion ($r_\varphi = 1/u_\varphi$) corresponds to the apsidal angle

$$\varphi = \pi/k = \pi + \Delta/2, \tag{17}$$

and it can be determined from the quadratic equation

$$\begin{gathered} u^2 + u + 1 = \frac{3}{2B}(u + 1 - 2A) \rightarrow \\ u^2 - (\frac{3}{2B} - 1)u + \frac{6A - 3}{2B} + 1 = 0 \rightarrow \\ u_\varphi = 0.65888124588,\ r_\varphi = 1.5177241821,\ \varphi = 3.14159290453. \end{gathered} \tag{18}$$

We therefore get an equation which is equivalent to (16):

$$\frac{d\theta}{du} = \frac{1}{\sqrt{\left(u - u_\varphi\right)\left[2A - u - u_\varphi + \frac{2B}{3}\left(u^2 + uu_\varphi + u_\varphi^2\right)\right]}}. \tag{19}$$

Our goal here is to ascertain the function $u(\theta)$ in the range $\theta \in [0, \varphi]$. To this end, we can combine the first-order differential equations (16) and (19), choosing a suitable intermediate point with polar coordinates $\left(\phi, r_\phi\right)$. Thus, integrating (16), we get

$$\theta = \int_{u_\theta}^{1} \frac{du}{\sqrt{(1-u)\left[u + 1 - 2A - \frac{2B}{3}\left(u^2 + u + 1\right)\right]}}, \; u_\theta \in \left[u_\phi, 1\right], \tag{20}$$

where $u_\phi = 1/r_\phi$. On the other hand, using (19), we can write

$$\varphi - \theta = \int_{u_\varphi}^{u_\theta} \frac{du}{\sqrt{\left(u - u_\varphi\right)\left[2A - u - u_\varphi + \frac{2B}{3}\left(u^2 + uu_\varphi + u_\varphi^2\right)\right]}}, \; u_\theta \in \left[u_\varphi, u_\phi\right]. \tag{21}$$

Let us fix r_ϕ by the condition $u''(\phi) = 0$, which corresponds to the minimum of the effective potential [14], p. 99

$$V^* = -\frac{L^2}{m}\left(Au - \frac{u^2}{2} + \frac{Bu^3}{3}\right), \tag{22}$$

i.e. to the solution of the quadratic equation

$$Bu^2 - u + A = 0 \to u_\phi = \frac{1}{2B} - \sqrt{\frac{1}{4B^2} - \frac{A}{B}}. \tag{23}$$

As $V^*(a) = V^*(b) = E$, it follows from (22) that

$$A - \frac{1 + u_\varphi}{2} + \frac{B}{3}\left[(1 + u_\varphi)^2 - u_\varphi\right] = 0. \tag{24}$$

Suppose

$$\frac{1 + u_\varphi}{2} = u_\phi + \Delta u. \tag{25}$$

Then, according to (22) and (23),

$$\begin{aligned} -\Delta u + \frac{u_\phi - A}{3} + \frac{B}{3}\left(8u_\phi \Delta u + 4\Delta u^2 - u_\varphi\right) = 0 \to \\ \Delta u^2 - (\frac{3}{4B} - 2u_\phi)\Delta u + \frac{u_\phi - A}{4B} - \frac{u_\varphi}{4} = 0. \end{aligned} \tag{26}$$

Introducing the numerical values (6) and (7) into (23) and (26), we get

$$u_\phi = 0.8294406220064744 \to \phi = 1.5707964632154577, \tag{27}$$

$$\Delta u = \frac{3}{8B} - u_\phi - \sqrt{\left(\frac{3}{8B} - u_\phi\right)^2 + \frac{u_\varphi}{4} - \frac{u_\phi - A}{4B}} = 9.3383 \cdot 10^{-10}. \tag{28}$$

We see that $\Delta u \neq 0$, differently from the pure Newtonian potential and the force field $V(r) = -a_1/r - a_2/r^2$, where $u_\phi = \left(1 + u_\varphi\right)/2$ and correspondingly, $\Delta u = 0$. The polar angle ϕ has been fixed by calculating the integrals (20) and (21) with $u_\theta = u_\phi$, and taking into account that the two independent estimations for ϕ must coincide to the desired accuracy (16 decimal digits). This is indeed the case, and the result is given in (27). However, as will be explained in the next subsection, achieving such a high accuracy is not at all trivial.

2.2. Evaluating the integrals

As can be seen, the integrands of (20) and (21) have a singularity at $u = 1$ and $u = u_\varphi$, respectively. A useful device in this situation is integration by parts. For (20) we can take $dv = \dfrac{du}{\sqrt{1-u}} \to v = -2\sqrt{1-u}$, so that the integral transforms to

$$\theta = \frac{2\left(1-u_\theta\right)}{u'_\theta} + \int_{u_\theta}^{1} \frac{\sqrt{1-u}\left[\frac{2B}{3}(1+2u)-1\right]du}{\left[u+1-2A-\frac{2B}{3}\left(u^2+u+1\right)\right]^{3/2}}, \tag{29}$$

where (15) was used. Analogously, taking $dv = \dfrac{du}{\sqrt{u-u_\varphi}} \to v = 2\sqrt{u-u_\varphi}$, (21) transforms to

$$\varphi - \theta = \frac{2\left(u_\theta-u_\varphi\right)}{u'_\theta} + \int_{u_\varphi}^{u_\theta} \frac{\sqrt{u-u_\varphi}\left[\frac{2B}{3}\left(u_\varphi+2u\right)-1\right]du}{\left[2A-u-u_\varphi+\frac{2B}{3}\left(u^2+uu_\varphi+u_\varphi^2\right)\right]^{3/2}}. \tag{30}$$

Thus, we got rid of the singularities, but by aiming at the highest accuracy, we can continue smoothening the integrands. Namely, the integral (29) can be rewritten as follows:

$$\theta = \int_{u_\theta}^{1} F_1(u)du + \frac{2\left(1-u_\theta\right)}{u'_\theta} + I_1,\ \theta \in [0,\phi],\ u_\theta \in \left[u_\phi, 1\right], \tag{31}$$

where

$$F_1(u) = \sqrt{1-u}\left[\frac{2B}{3}(1+2u)-1\right] \times\left[\frac{1}{\left[u+1-2A-\frac{2B}{3}\left(u^2+u+1\right)\right]^{3/2}} - \frac{1}{[2(1-A-B)]^{3/2}}\right] \tag{32}$$

and

$$I_1 \equiv \frac{1}{[2(1-A-B)]^{3/2}} \int_{u_\theta}^{1} \sqrt{1-u}\left[\frac{2B}{3}(1+2u)-1\right]du. \tag{33}$$

The idea is simple. The second term in the square brackets of (32) is the limit value of the first term, as $u \to 1$. As can be seen, we subtracted I_1 from the initial expression for ϕ. Of course, as shown by formula (31), the same quantity (I_1) must also be added to (31). A good point is that I_1 can be evaluated analytically:

$$I_1 = -\frac{\left(1-u_\theta\right)^{3/2}}{3\,[2(1-A-B)]^{3/2}}\left[2-4B+\frac{8B\left(1-u_\theta\right)}{5}\right]. \tag{34}$$

Another good point is that $F_1(u)$ is a smooth function, perfectly suitable for numerical integration.

The integrand of (30) can be smoothened in a similar way. The result is as follows:

$$\theta = \varphi - \left[\int_{u_\varphi}^{u_\theta} F_2(u)du + \frac{2\left(u_\theta-u_\varphi\right)}{u'_\theta} + I_2\right],\ \theta \in [\phi,\varphi],\ u_\theta \in \left[u_\varphi, u_\phi\right], \tag{35}$$

$$F_2(u) = \sqrt{u-u_\varphi}\left[\frac{2B}{3}\left(u_\varphi+2u\right)-1\right] \times\left[\frac{1}{\left[2A-u-u_\varphi+\frac{2B}{3}\left(u^2+uu_\varphi+u_\varphi^2\right)\right]^{3/2}} - \frac{1}{\left[2(A-u_\varphi+Bu_\varphi^2)\right]^{3/2}}\right], \tag{36}$$

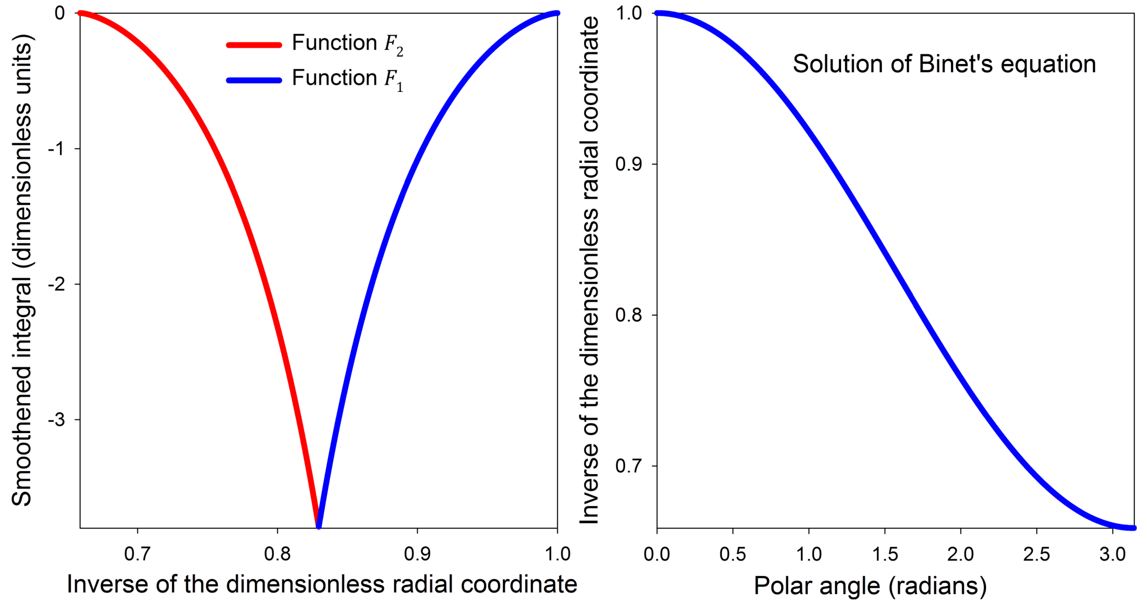

Fig. 1. Smoothened integrands for the numerically solved Binet's equation. The functions $F_1(u)$ and $F_2(u)$ are given by (32) and (35), respectively. The curves look symmetric relative to the bottom point (ϕ, u_ϕ), but this is not quite the case, as $\Delta u \neq 0$, according to (28). The overall result of the numerical integration is shown on the right-side graph.

$$I_2 \equiv \frac{\left(u_\theta - u_\varphi\right)^{3/2}}{3\left[2(A - u_\varphi + Bu_\varphi^2)\right]^{3/2}}\left[\frac{8B\left(u_\theta - u_\varphi\right)}{5} - 2 + 4Bu_\varphi\right]. \tag{37}$$

Both smoothened integrands, $F_1(u)$ and $F_2(u)$, are shown in Fig. 1. Thereafter, these functions have been integrated numerically by using the adaptive Simpson's method (see, e.g. [16]). Aiming at the highest accuracy, all computations have been performed in the high-precision programming environment UBASIC (see, e.g. [17]).

As the radial coordinate is a periodic function, we only need to calculate the relativistic orbit for the interval $\theta \in [0, \varphi]$. This has been done with utmost accuracy, by dividing the full range of integration $u_\theta \in \left[u_\varphi, 1\right]$ into 40 000 subintervals. If the function $r(\theta)$ for any $\theta \in [0, \varphi]$ is known, then the value of this function at an arbitrary polar angle θ can be determined as follows:

$$\theta = 2\varphi \cdot (n + x), \;\; n = \left[\frac{\theta}{2\varphi}\right], \;\; x = \frac{\theta}{2\varphi} - \left[\frac{\theta}{2\varphi}\right] \in [0, 1),$$

where the square brackets denote the integer part of the argument. For any $x \in [0, 1)$, we can define another number related to an angle $\Phi \in [0, 1)$:

$$y = \begin{cases} x, \;\; \text{if } x \leq 1/2, \\ 1 - x, \;\; \text{if } x \geq 1/2 \end{cases} \;\; \rightarrow \Phi = 2\varphi \cdot y.$$

Thus, $r(\theta) = r\left(\Phi\right)$.

3. Analytic approximation of Mercury's relativistic trajectory

As explained in Section 1, the first-order perturbational solution to the relativistic Binet's equation is given by (8), where the constants A_0, B_0 and k are explicitly determined by the basic parameters A and B. This is the simplest model that approximates the overall trajectory with reasonable accuracy, the largest discrepancy (at aphelion) being 14.24 km [11]. However, aiming at a much higher accuracy, we are now going to slightly modify (8), assuming that

$$u(\theta) = A_1 \cos\left(k\theta\right) + B_1,$$

where A_1 and B_1 can be treated as variable parameters. Moreover, k does not need to be a constant but may be a slowly varying function $k\left(\theta\right)$.

Let us recall that (8) is the **exact solution** of Binet's equation for a central potential of another type, (12). Hopefully, a better approximation is obtained if we determine the coefficients A_1 and B_1 from the real (relativistic) perihelion and aphelion distances. To this end, we can apply a slightly modified version of formula (11). Namely,

$$A_1 = \frac{r_\varphi - a_p}{2r_\varphi \cdot a_p}, \ B_1 = \frac{a_p + r_\varphi}{2r_\varphi \cdot a_p}. \tag{38}$$

In dimensionless units, the perihelion $a_p = 1$, while the aphelion r_φ is given in (18). Thus,

$$A_1 = 0.1705593770597, \ B_1 = 0.8294406229403, \tag{39}$$

and we assume that these coefficients are fixed and remain the same for all four models described in the next subsection. In addition, we assume that the function $u(\theta)$ can be identified with the numerical solution of (5), which was ascertained in the previous subsection. It means that

$$k(\theta) = \frac{\arccos\left[\dfrac{u(\theta) - B_1}{A_1}\right]}{\theta}, \tag{40}$$

where the right side is a known function. This can be viewed as a kind of inverse problem: our goal now is to find a simple but reliable analytic expression for the function $k(\theta)$. Aiming at that goal, we propose several simple models.

3.1. Analytic expressions for the function $k(\theta)$

Model A. This is the simplest case when k is assumed to be a constant given by (10):

$$k = k_0 \equiv \frac{\pi}{\varphi} = 0.999999920123. \tag{41}$$

Thus, the trajectory can be calculated by the formula

$$u_A(\theta) = A_1 \cos\left(k_0\theta\right) + B_1, \tag{42}$$

where the subscript refers to the model under study. The result, in comparison with the numerical solution of equation (5), can be seen in Fig. 2. Quite remarkably for this simple model, the largest deviation from the relativistic orbit is only 65 m.

Model B. Suppose $k(\theta)$ is a linear function:

$$k(\theta) = k_0 + \alpha_0(\varphi - \theta), \tag{43}$$

where k_0 is the constant given in (41), φ is the apsidal angle given in (18) and α_0 is a fitting parameter to be determined. For example, we can fix α_0 by the condition

$$u_\phi = A_1 \cos\left\{\left[k_0 + \alpha_0(\varphi - \phi)\right]\phi\right\} + B_1, \tag{44}$$

where ϕ and u_ϕ are given in (27). Thus,

$$\alpha_0 = \frac{\arccos\left(\dfrac{u_\phi - B_1}{A_1}\right) - k_0\phi}{\phi(\varphi - \phi)} = -2.21897771258 \cdot 10^{-9}, \tag{45}$$

and the trajectory for this model reads

$$u_B(\theta) = A_1 \cos\left\{\left[k_0 + \alpha_0(\varphi - \theta)\right]\theta\right\} + B_1. \tag{46}$$

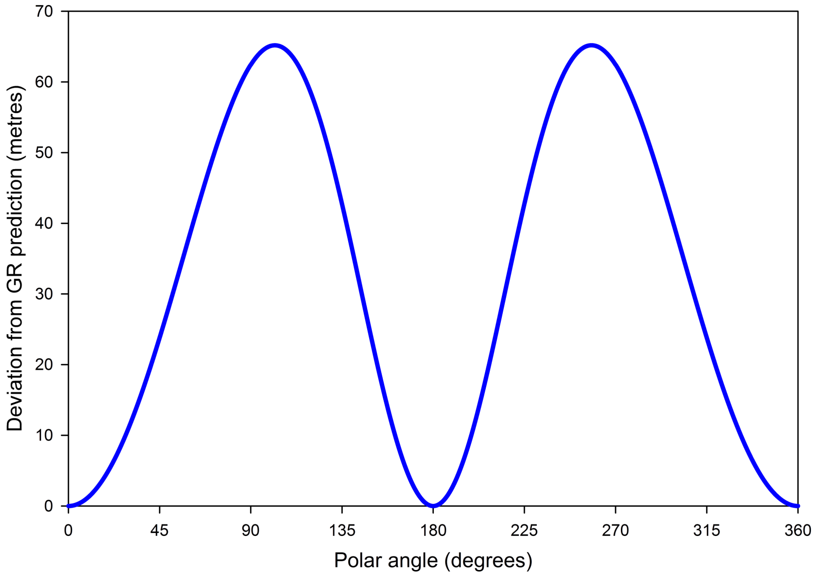

Fig. 2. Model A: the difference between the numerical solution of Binet's equation (5) and the trajectory according to formula (42), with the parameters given in (39) and (41).

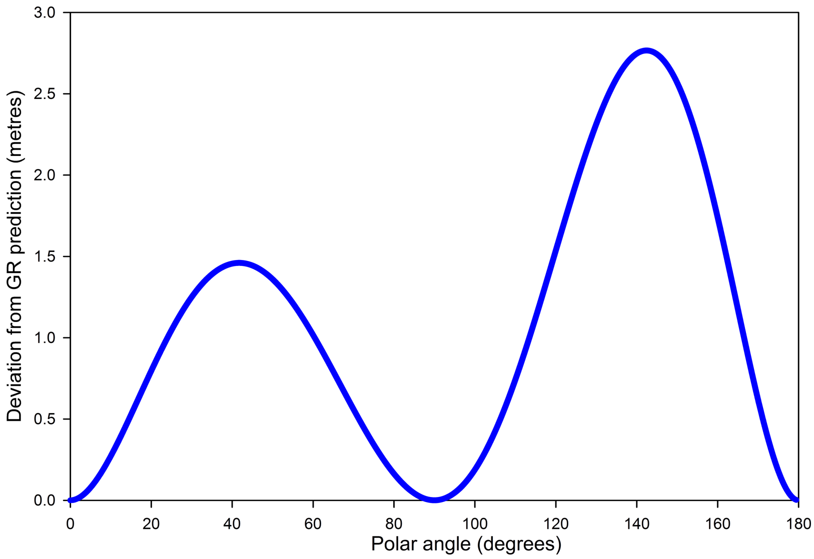

Fig. 3. Model B: the numerical solution of Binet's equation (5) in comparison with the trajectory according to formula (46).

As can be seen in Fig. 3, (46) gives a much better approximation to the relativistic orbit: the discrepancy being less than 3 m.

Model C. To get an even better approximation to the real orbit, suppose $k(\theta)$ is a simple rational function with two fitting parameters, α and β:

$$k(\theta) = k_0 + \frac{\alpha \cdot (\varphi - \theta)}{\varphi + \beta \cdot \theta \cdot (\varphi - \theta)}. \tag{47}$$

Thus,

$$u_C(\theta) = A_1 \cos\left\{\left[k_0 + \frac{\alpha \cdot (\varphi - \theta)}{\varphi + \beta \cdot \theta \cdot (\varphi - \theta)}\right] \cdot \theta\right\} + B_1, \tag{48}$$

where A_1, B_1 and k_0 are the constants given in (39) and (41). We see that $u_C(0) = 1$ and $u_C(\varphi) = u_\varphi$, as needed.

The derivative of (48) reads

$$u' = -A_1 \sin\left[k(\theta)\,\theta\right]\left[k(\theta) + k'(\theta)\,\theta\right], \tag{49}$$

where

$$k'(\theta) = -\frac{\alpha}{\varphi + \beta\cdot\theta\cdot(\varphi-\theta)} - \frac{\alpha\cdot\beta\cdot(\varphi-\theta)\cdot(\varphi-2\theta)}{\left[\varphi+\beta\cdot\theta\cdot(\varphi-\theta)\right]^2}. \tag{50}$$

As $k(0) = k_0 + \alpha$, it follows that

$$u''(0) = -A_1 \cos\left[k(\theta)\,\theta\right]\left(k_0+\alpha\right)^2, \tag{51}$$

and therefore,

$$\left(u''+u\right)\big|_{\theta=0} = 1 - A_1\left(k_0+\alpha\right)^2. \tag{52}$$

On the other hand, as $u(0) = 1$, it follows from (5) that

$$\left(u''+u\right)\big|_{\theta=0} = A + B. \tag{53}$$

Thus, equating (53) with its approximant (52), we get

$$\alpha = \sqrt{\frac{1-A-B}{A_1}} - k_0 = -5.475095605182012\cdot 10^{-9}. \tag{54}$$

There remains to determine the second fitting parameter β. To this end, analogously to the constraint (44), we assume that equation (48) predicts the correct value for u_ϕ, i.e.

$$\arccos\left(\frac{u_\phi - B_1}{A_1}\right) - k_0\phi = \frac{\alpha\cdot\phi\cdot(\varphi-\phi)}{\varphi+\beta\cdot\phi\cdot(\varphi-\phi)}. \tag{55}$$

From this we obtain

$$\beta = \frac{\alpha}{\arccos\left(\dfrac{u_\phi - B_1}{A_1}\right) - k_0\phi} - \frac{\varphi}{\phi\cdot(\varphi-\phi)} = -0.27324119900454. \tag{56}$$

As both fitting parameters are fixed, we can calculate the trajectory according to (48). As shown in Fig. 4, the result is practically indistinguishable from the numerical solution of the relativistic Binet's equation. This is in agreement with constraint 2 stated in Section 1. However, it would be desirable to determine all model parameters without actually solving Binet's equation. This was not the case for the important reference angle ϕ, which corresponds to the minimum of the effective potential, and has been determined from the numerical solution of (5). Fortunately, somewhat surprisingly, the following simple formula holds:

$$\phi = \varphi/2 - 2\alpha, \tag{57}$$

where φ and α are given in (18) and (54), respectively. Strictly speaking, (57) is an approximate relation, but the approximation is so good that we can use here the equality sign instead of $\approx$. We shall prove this now.

Proof. Let us assume that in a tiny range of polar angles around ϕ (including $\varphi/2$), (48) gives a highly reliable prediction of the real orbit. It then follows that

$$u_{\varphi/2} = -A_1 \sin\left(\frac{\alpha\varphi}{4+\beta\varphi}\right) + B_1 = 0.82944062387413. \tag{58}$$

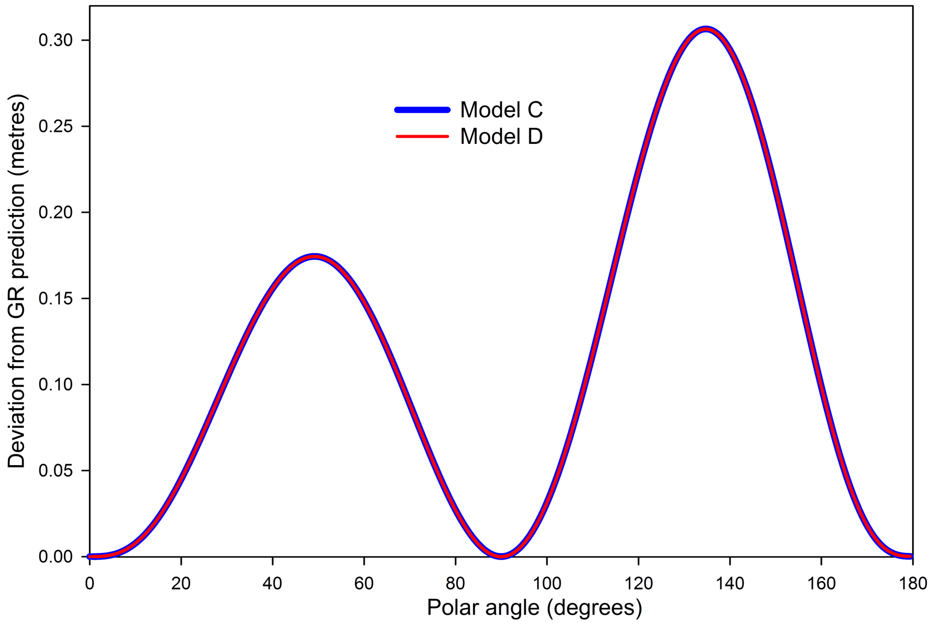

Fig. 4. Models C and D: the numerical solution of Binet's equation (5) in comparison with the trajectories according to (48). For model C, the parameter ϕ was determined numerically (see the explanations at the end of Section 2), while for model D, this parameter was fixed by (57). As can be seen, the predictions of models C and D are almost identical, both giving a very good approximation to the real trajectory.

On the other hand, taking into account that $\phi \approx \varphi/2$, we can use the Taylor expansion

$$u_{\varphi/2} = u_\phi + u'_\phi \cdot (\varphi/2 - \phi) + ...,$$

where higher-order terms can be ignored, as $u''_\phi = 0$ and $(\varphi/2 - \phi)^k$ for $k = 3, 4, ...$ is a very small quantity. Thus, using (58), (18), (15) and (27), we get

$$\phi = \varphi/2 + \frac{u_\phi - u_{\varphi/2}}{u'_\phi} = \varphi/2 - 2 \cdot \left(-5.475091188 \cdot 10^{-9}\right) = \varphi/2 - 2\,(\alpha + \Delta\alpha),$$

where $\Delta\alpha = 4.417 \cdot 10^{-15}$. We see that $\Delta\alpha$ is indeed a very small quantity, which completes the proof. How could we interpret this surprising but very useful result? A reasonable explanation seems to be that (48) provides a very good approximation, so that the fitting parameter α can be explicitly related to the important characteristics ϕ and φ of the real relativistic trajectory.

Model D. Using the obtained result, we can slightly modify model C. The basic formula (48) remains the same, as well as the fitting parameter α determined by (54). Thereafter, one uses (57) to get

$$\phi = 1.5707964632154628, \tag{59}$$

which is slightly different but, in fact, almost indistinguishable from the value given in (27). Finally, using (56) and (59), we obtain

$$\beta = -0.2732428582076941. \tag{60}$$

Inserting these modified parameters into (48), we get another approximation to the relativistic trajectory. As expected and explicitly demonstrated in Fig. 4, the predictions of models C and D practically coincide, and they both give a very good approximation to the numerically calculated relativistic orbit. Analogously, inserting (57) into (45), one gets a marginally modified value for the fitting parameter α_0, which has almost no effect on the trajectory $u_B(\theta)$.

3.2. Conceivable force field for model D

Probably the most unexpected result of this work is the simple formula (57) that connects three parameters of rather different kind. Indeed, the apsidal angle φ is an important characteristic of the real relativistic orbit, and α is a fitting parameter for models C and D. The third quantity, the polar angle ϕ, corresponds to the minimum of the real effective potential, but according to (57), it is also a fitting parameter for model D. Therefore, to provide an additional argument for the validity of (57), let us calculate the central force that corresponds to

$$u_D(\theta) = A_1 \cos[k(\theta)\cdot\theta] + B_1, \tag{61}$$

where A_1 and B_1 are given in (39) and the function $k(\theta)$ is defined by formula (47) with the parameters k_0, φ, α and β given in (41), (18), (54) and (60), respectively. Note that all these fitting parameters are uniquely fixed by the basic parameters A and B given in (6) and (7), in accordance with constraint 3 stated in Section 1. Moreover, there is no need to solve Binet's equation (5) in order to fix the function $k(\theta)$ in (61). This hugely saves time and is the main reason why model D (not C) is additionally tested in this subsection.

To begin the analysis, let us fix the first and the second derivatives of (61):

$$\begin{aligned} u_D' &= -A_1 \sin[k(\theta)\,\theta]\,\big[k(\theta) + k'(\theta)\,\theta\big], \\ u_D'' &= -A_1 \cos[k(\theta)\,\theta]\,\big[k(\theta) + k'(\theta)\,\theta\big]^2 - A_1 \sin[k(\theta)\,\theta]\,\big[2k'(\theta) + k''(\theta)\,\theta\big], \end{aligned} \tag{62}$$

where

$$\begin{aligned} k'(\theta) &= -\frac{\alpha}{\varphi + \beta\cdot\theta\cdot(\varphi-\theta)} - \frac{\alpha\cdot\beta\cdot(\varphi-\theta)\cdot(\varphi-2\theta)}{[\varphi + \beta\cdot\theta\cdot(\varphi-\theta)]^2}, \\ k''(\theta) &= \frac{\alpha\cdot\beta\cdot(4\varphi-6\theta)}{[\varphi + \beta\cdot\theta\cdot(\varphi-\theta)]^2} + \frac{2\alpha\cdot\beta^2\cdot(\varphi-\theta)\cdot(\varphi-2\theta)^2}{[\varphi + \beta\cdot\theta\cdot(\varphi-\theta)]^3}. \end{aligned}$$

Thus, according to Binet's equation (3),

$$\begin{aligned} -\frac{mr^2}{L^2}F(r) = A_1 \cos[k(\theta)\,\theta]\left\{1 - \big[k(\theta) + k'(\theta)\,\theta\big]^2\right\} \\ -A_1 \sin[k(\theta)\,\theta]\,\big[2k'(\theta) + k''(\theta)\big] + B_1. \end{aligned} \tag{63}$$

The function $F(r)$ consists of two parts:

$$F(r) = -\frac{GMm}{r^2} + F_D, \tag{64}$$

where the first term is Newton's gravitational force and $F_D(r)$ is the additional force we are seeking. As

$$-\frac{mr^2}{L^2}\cdot\left(-\frac{GMm}{r^2}\right) = A,$$

we can separate the second term of the corresponding Binet's equation in order to make a comparison with the relativistic term Bu^2 of equation (5):

$$\begin{aligned} B_D u_D^2 \equiv -\frac{mr_D^2}{L^2}F_D = A_1 \cos[k(\theta)\,\theta]\left\{1 - \big[k(\theta) + k'(\theta)\,\theta\big]^2\right\} \\ -A_1 \sin[k(\theta)\,\theta]\,\big[2k'(\theta) + k''(\theta)\big] + B_1 - A. \end{aligned} \tag{65}$$

The result of the comparison is shown in Fig. 5. As expected, the functions B/r^2 and B_D/r_D^2 nearly coincide, which confirms the validity of model D.

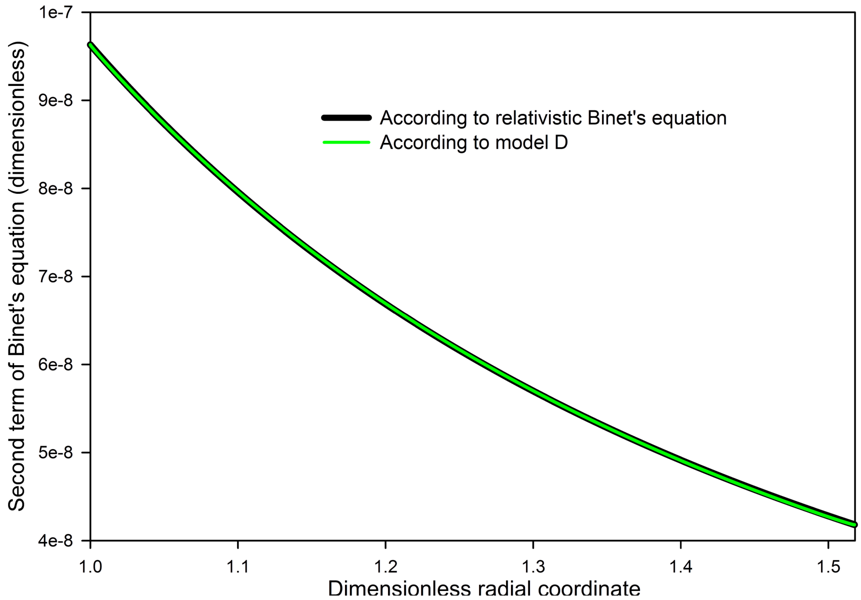

Fig. 5. A comparison between the second term of the relativistic Binet's equation B/r^2 and the corresponding term B_D/r_D^2 in the frame of model D, according to formula (65).

4. Conclusion

Although the relativistic Binet's equation cannot be solved analytically, one can construct a highly reliable analytic approximant to that solution. In this article, we proposed four different models for this purpose. The simplest and the most unpunctual of them is model A based on formula (42), which is, in fact, the exact solution for a potential $V(r) = -a_1/r - a_2/r^2$. The coefficients a_1 and a_2 can be easily evaluated, but this effort is unnecessary because the constants A_1, B_1 and k_0 are explicitly related to the parameters of the real relativistic orbit. In particular, the aphelion of approximant (42) equals the real aphelion given by (18). This is an important nuance that makes (42) quite reliable, as it predicts the correct positions of both the perihelion and the aphelion. Unsurprisingly, the largest discrepancy (but only 65 m; see Fig. 2) occurs near $\theta = \varphi/2$.

Compared with model A, an additional constraint is set for models B, C and D: the model must correctly predict the position of the point (ϕ, u_ϕ). The inverse of the minimum of the effective potential $u_\phi = 1/r_\phi$ is given by (23), but the corresponding polar angle ϕ can only be determined, strictly speaking, by very accurately calculating the integrals (20) and (21) for $u_\theta = u_\phi$. Fortunately, as we proved, a simple formula (57) can be used, which predicts the correct value for ϕ with a very high degree of accuracy. This way we easily get the necessary reference point between the perihelion and the aphelion. As a result, a much better approximation to the real relativistic trajectory is achieved.

Another innovation compared with model A concerns the argument of the cosine function in the basic formula $u(\theta) = A_1 \cos(k\theta) + B_1$. Namely, in the frame of models B, C and D, k is not a constant but a function of the polar angle θ. The function $k(\theta)$ is built up in such a way that it ensures the correct position of the perihelion and the aphelion. Model B contains a single fitting parameter α_0, which should fit with the position of the third reference point (ϕ, u_ϕ). Its value given in (45) is based on the numerical estimation (27). Alternatively, using (57), we get the value

$$\alpha_0 = \frac{\arccos\left(\dfrac{u_\phi - B_1}{A_1}\right) - k_0\phi}{\phi(\varphi - \phi)} = -2.218979779535 \cdot 10^{-9}, \tag{66}$$

which only marginally differs from (45). Thus, it does not matter which of these values, (45) or (66), is inserted into (44): the real trajectory is approximated with the precision better than 3 m.

Models C and D are practically identical. They include two fitting parameters, α and β, where α is the same in both models and is given by (54). The value of β depends on the parameter ϕ, which is marginally different for models C and D. On the basis of simplicity, the preference should certainly be given to model D because then there is actually no need to solve Binet's equation (5). Indeed, to apply (61), one first uses (18) to determine the aphelion r_φ. The next step is to fix the coefficients A_1

and B_1 according to (38). The constant $k_0 = \pi/\varphi$ is determined by the apsidal angle (17), the fitting parameter α is obtained from (54), and the parameters ϕ and β for model D are given in (59) and (60), respectively. Thus, in presumption that the basic parameters A and B are known, all parameters for model D are uniquely determined, and one can use (61) to get an excellent approximation to the real relativistic trajectory. The conclusion is paradoxical: **the highly reliable solution to the relativistic Binet's equation can be obtained without actually solving this equation!**

In this context, we have to recall once again that the success of model D is based on formula (57), which enables to easily fix the third reference point (ϕ, u_ϕ) in addition to the perihelion and the aphelion. Obviously, if two nearly elliptical curves have three common points not close to each other, these curves would be relatively close everywhere. Thus, unsurprisingly, their largest difference is less than 31 cm. Of course, there is no need for such an extreme precision, but the real point is that there is also no need to solve the relativistic trajectory equation. Instead, one can use a simple analytic formula (61) for this trajectory. Elaborating model D, which provides optimal balance between simplicity and accuracy, may be considered the main result of this work.

To test the actual quality of this model, one needs a highly reliable comparison basis. This was obtained by solving the relativistic Binet's equation numerically to a high degree of accuracy. The corresponding data file is available as a supplementary material for this article (online resource).

The proposed approach was applied to study the orbit of Mercury, which does not mean that the obtained results are somehow specific to Mercury. On the contrary, the principles of the theoretical analysis remain the same for any other planet or celestial body in the relativistic force field. It would therefore be interesting to perform an analogous study for another planet, e.g. for Venus whose perihelion shift per orbit, $\Delta = 2.572418 \cdot 10^{-7}$rad [12], is not so different from that of Mercury.

Data availability statement

Online resource: the data supporting this work are available in the spreadsheet Mercury-GRdata.xlsx, which can be accessed at https://osf.io/er7hk/?view_only=fa7e4f75c3984b2e9ab634df8ff6283e. It contains the numerical solution of the relativistic Binet's equation from $\theta = 0$ to φ with step $\varphi/40000$.

Acknowledgements

I am grateful to the reviewers for their careful work and useful suggestions for improving the quality and readability of this article. The publication costs of this article were covered by the Estonian Academy of Sciences.

References

1. Binet, J. M. Mémoire sur la détermination des orbites des planètes et des comètes (Memoir on the determination of the orbits of planets and comets). *Journal de l'École Polytechnique*, 1831, **13**, 249–288.
2. Newton, Sir I. *Mathematical Principles of Natural Philosophy and his System of the World* (translated by Motte, A., 1729). 8th printing. University of California Press, 1974.
3. Whittaker, E. T. *A Treatise on the Analytical Dynamics of Particles and Rigid Bodies*. 2nd ed. Cambridge University Press, 1917.
4. Einstein, A. Erklärung der Perihelbewegung des Merkur aus der allgemeinen Relativitätstheorie (Explanation of the perihelion motion of Mercury from the general theory of relativity). *König. Preuss. Akad. Wiss.*, 1915, **XLVII**, 831–839. An English translation is available at: http://einsteinpapers.press.princeton.edu/vol6-trans/124
5. Saca, J. M. An exact solution to the relativistic advance of perihelion: correcting the Einstein approximation. *Astrophys. Space Sci.*, 2008, **315**, 365. https://doi.org/10.1007/s10509-008-9785-8
6. Mercury facts. https://science.nasa.gov/mercury/facts/ (accessed 2025-04-30).
7. D'Inverno, R. *Introducing Einstein's Relativity*. Clarendon Press, Oxford, 1992.
8. Thornton, S. T. and Marion, J. B. *Classical Dynamics of Particles and Systems*. 5th ed. Brooks/Cole, 2004.
9. Shahid-Saless, B. and Yeomans, D. K. Relativistic effects on the motion of asteroids and comets. *Astron. J.*, 1994, **107**, 1885–1889.
10. Schwarzschild, K. Über das Gravitationsfeld eines Massenpunktes nach der Einsteinschen Theorie (On the gravitational field of a point-mass according to Einstein's theory). *Sitzungsberichte der Königlich Preussischen Akademie der Wissenschaften*, 1916, **7**, 189–196.
11. Selg, M. An interesting class of exact solutions to Binet's equation, with references to Newton's and Einstein's theories of gravity. *Eur. J. Phys.*, 2025, **46**, 015002.
12. Andersen, P. B. What GR predicts for the perihelion advance of planets. 2023. https://www.paulba.no/pdf/GRPerihelionAdvance.pdf
13. Simon, J. L., Bretagnon, P., Chapront, J., Chapront-Touze, M., Francou, G. and Laskar, J. Numerical expressions for precession formulae and mean elements for the Moon and the planets. *Astron. Astrophys.*, 1994, **282**, 663–683.
14. Cheng, T.-P. *Relativity, Gravitation and Cosmology*. Oxford University Press, 2005.
15. Runge–Kutta method. https://keisan.casio.jp/exec/system/1548123555 (in Japanese) (accessed 2025-04-30).
16. Plaskota, L. Automatic integration using asymptotically optimal adaptive Simpson quadrature. *Numer. Math.*, 2015, **131**, 173–198.
17. UBASIC. https://en.wikipedia.org/wiki/UBASIC

Lihtne ja usaldusväärne analüütiline lähend relativistliku Binet′ võrrandi numbrilisele lahendile – rakendus Merkuurile

Matti Selg

Mittelineaarne trajektoori võrrand (Binet′ võrrand), mis kirjeldab osakese liikumist relativistlikus jõuväljas, on lahendatav ainult numbriliselt või alternatiivina häiritusteoreetilise lahendusskeemi abil. Viimast kasutas 1915. aastal Albert Einstein, tuletades kuulsa valemi Merkuuri periheeli anomaalse pretsessiooni kindlakstegemiseks. Käesoleva artikli fookuses ei ole periheeli pretsessioon, vaid Merkuuri relativistlik orbiit tervikuna, mis on arvutatud numbriliselt 16 kümnendkoha täpsusega. See on hädavajalik võrdlusbaas, et saavutada töö peaeesmärki – tuletada lihtne analüütiline valem, mis oleks perfektses kooskõlas tegeliku relativistliku trajektooriga. Analüüsitakse mitut erineva täpsusastmega mudelit ning peaeesmärk saavutatakse edukalt. Ühtlasi selgub, et kolmandas jaotises kirjeldatava mudeli D sobitusparameetrid on leitavad Binet′ võrrandit lahendamata. Järeldus on paradoksaalne: relativistliku Binet′ võrrandi lahendi saab trajektoori mistahes punktis väga täpselt kindlaks teha (suurim kõrvalekalle on umbes 30 cm) seda mittelineaarset diferentsiaalvõrrandit tegelikult lahendamata.